AMERICAN JOURNAL OF DIAGNOSTIC IMAGING, 2022
VOL 8, NO. 1, PAGE 27–33
10.5455/ajdi.20210504082116

ORIGINAL ARTICLE

Open Access

Differentiating swine flu from other viral pneumonia on chest computed tomography with emphasis on anterior pericardial thickening

Rajesh Ghosh[1], Nilu Malpani Dhoot[1], Usha Goenka[1], Srijita Ghosh[1], Somali Ghosh[1]
[1]Department of Radiology and Imaging, Apollo Gleneagles Hospital, Kolkata, India

ABSTRACT

Objective: To establish utility of anterior pericardial (AP) thickening for Influenza A Hemagglutinin 1 Neuraminidase 1 (H1N1) on computed tomography (CT) thorax.
Methods: A prospective study was carried out on 385 patients with a positive comprehensive viral panel test from December 2018 to January 2020. Of this, 102 patients positive for H1N1 formed the study group. The control group consisted of the remaining 248 patients with a positive comprehensive viral panel other than H1N1. Thirty-five patients were excluded from the study, as they were positive for two or more viruses. The CT scan of these patients was evaluated for various morphological findings indicating viral infection and the presence of the "AP" sign. The AP sign was considered as positive when the pericardium was thickened focally or diffusely, with thickness more than 4 mm.
Results: Ground glass opacity was the most prevalent finding in viral pneumonia. The AP sign, when present, could identify 72.5% of patients with swine flu. It was absent in 49% of patients with other viral infections and was an effective assertor of SF ($p < 0.0004$). The sign had a specificity of 48%, a positive predictive value of 36%, a negative predictive value of 81%, and an accuracy of 55.4%.
Conclusion: The absence of AP sign-on high resolution computed tomography (HRCT) chest has a high negative predictive value for SF. It can be used as an additional diagnostic tool in differentiating SF from other OV infections on HRCT.

ARTICLE HISTORY

Received May 04, 2021
Accepted January 03, 2022
Published January 28, 2022

KEYWORDS

Swine flu, CT chest, pericardial thickening, viral pneumonia

Introduction

An infectious viral disease, Influenza A, has many subtypes. Hemagglutinin 1 Neuraminidase 1 (H1N1) is one of them. Widespread disease in pigs worldwide, H1N1 swine influenza, is also known as swine flu (SF). People who work near pigs may sometimes acquire the disease (Zoonotic SF). SF influenza viruses can potentially cause infections in humans if antigenic characteristics of the virus change through reassortment [1]. Even when this happens, transmission from human-to-human is generally inefficient. Influenza A pandemics such as the ones in 1918 and 2009 can occur if the transmission from person-to-person becomes possible due to genetic mutation [2]. Clinical manifestations cannot differentiate SF from any other viral (OV) fever [3]. The features could vary from minor upper respiratory tract symptoms to severe lower respiratory symptoms or life threatening like adult respiratory distress syndrome requiring admission to the intensive care unit. The comprehensive viral panel is a reasonably accurate test used to diagnose SF [4]. COVID-19 is not included in comprehensive viral panel. The other common biochemical findings are increased serum lactate dehydrogenase levels, increased C-reactive protein levels, increased serum creatine kinase levels, lymphopenia, and thrombocytopenia. Elevated lactate dehydrogenase levels are related to disease severity and the need for intensive care unit (ICU) admission [5,6]. Chest X-ray is useful in identifying the approach in most of the affected patients [7]. However, high resolution computed tomography (HRCT) is useful in defining the extent of pulmonary involvement and associated complications especially when there is a failure to respond to conventional treatment and in suspected superadded infections [8]. The radiological assessment of the patient can

Contact Nilu Malpani Dhoot drniludhoot@gmail.com Apollo Gleneagles Hospital, Kolkata, India.

© 2022 The Authors. This is an open access article under the terms of the Creative Commons Attribution NonCommercial ShareAlike 4.0 (https://creativecommons.org/licenses/by-nc-sa/4.0/).

contribute significantly to the management of the disease, especially in patients with forme fruste or atypical clinical manifestations [9]. Therefore, the knowledge of the imaging features is essential in clinical practice. The present study aimed to prospectively analyze HRCT thorax scans of patients with confirmed H1N1 infection in terms of standard imaging features and also to establish the value of anterior pericardial (AP) diagnostic sign indicating swine influenza. The study also compares various CT features and AP sign in OV infections in the comprehensive respiratory viral panel.

Materials and Methods

Patient population

A prospective study was performed on 385 symptomatic patients having a positive comprehensive viral panel referred for CT at a tertiary referral hospital. The study period was from December 2018 to January 2020. Out of these 385 cases, 35 patients were excluded as more than one virus infected them. Therefore, there were total of 350 patients which formed our study group satisfying all the inclusion criteria.The study group consisted of consecutive 102 adult patients with positive comprehensive respiratory viral panel for swine influenza. These patients also had other biochemical parameters positive, linking them to SF like increased serum lactate dehydrogenase levels or lymphopenia or thrombocytopenia. The control group consisted of 248 consecutive adult patients with positive comprehensive respiratory viral panel for other viruses. Of these, 22.3% were entero rhinovirus, 19.4% adenovirus, 14.4% coronavirus, 10.3% parainfluenza virus, 8.8% metapneumovirus, 7% influenza B, and the rest of the viruses made up a small percentage. The rest of the viruses forming a small percentage consisted of *Bordetella pertussis*, Chlamydophila pneumonia, *Mycoplasma* pneumonia, *Bordetella parapertusis*, and middle east respiratory syndrome corona virus. Informed consent was available for all patients, and clearance was taken from the hospital's ethical committee.

CT protocol

All CT examinations were obtained with the Aquilion Prime 160 CT system (Toshiba, Tokyo, Japan) or Philips Brilliance 16 CT system (Philips, Amsterdam, Netherlands) helical mode scanners. The CT machines were fumigated after each scan. All safety measures were taken to control cross infection. Both patients and the technician wore a mask. Distant instructions were given to the patients whenever feasible. The tube voltage was at 120 kVp, and tube current was set to automatic, which modulated the dose according to the patient size. The images were obtained from the thyroid gland level up to the level of the pancreas. No contrast was administered. The scan was captured in the end-inspiratory phase, whenever possible for the patient to hold breath adequately. Expiratory scan and prone sections were taken where needed. The slice thickness was 8 mm.

The images were analyzed by three senior radiologists with more than 10 years of experience in chest radiology, in both lung (window width 1,500 HU; level, −700 HU) and mediastinal (window width 350 HU; level, 40 HU) settings. Multiplanar reconstructions in the coronal, sagittal, and oblique planes were also performed and read in addition to the axial sections. The radiologist was aware that the patient had a viral infection with one of the comprehensive respiratory panel viruses; however, they were blinded to the identity of the virus. The following criteria were analyzed at CT.

The anterior pericardium was assessed for diffuse regular and uniform thickening or focal thickening. AP sign was considered as positive when diffuse or focal pericardial thickening of more than 4 mm was clearly identified in the anterior pericardium without pericardial effusion. The sign was taken as negative in the presence of pericardial effusion. Pericardial effusion was confirmed on echocardiography. Eighteen patients had pericardial effusion, of which four had SF infection.

The HRCT was also assessed for the presence of ground-glass opacities (GGO), consolidation, nodular infiltrates, tree in bud pattern, septal thickening, peribronchial cuffing, reticulation, and architectural distortion. Hilar, mediastinal lymphadenopathy, and pleural abnormalities were also evaluated.

GGO was defined as hazy, ill-defined areas of increased attenuation without obscuration of underlying vessels. When GGO was associated with septal thickening, it was called a crazy-paving pattern. Consolidation was defined as homogenous opacification of the lung parenchyma with obscuration of the underlying vessels with or without air bronchogram. Nodular infiltrates were defined as randomly distributed tiny rounded opacities. The tree in bud pattern was identified as multiple areas of centrilobular nodules with a linear branching pattern. Peribronchial cuffing was an abnormal thickening of bronchial walls. Architectural distortion was due to subpleural

fibrosis. Reticulation was identified as linear opacities forming a mesh-like pattern [10].

The involvement of the lung was categorized as unilateral or bilateral, symmetric, or asymmetric. The distribution pattern was noted as focal, multifocal, or diffuse. A single opacity as a focal pattern of involvement, multiple opacities in multiple lobes as a multifocal pattern, and widespread confluent opacities were noted as a diffuse pattern of involvement. The predominant mode of distribution was also noted as central, peribronchovascular, subpleural, or lobar (upper, middle, or lower). The CT features of SF and OV infections of the comprehensive viral panel were then compared and analyzed.

Statistical analysis

Data analysis was carried out using the commercially available Statistical Package for the Social Sciences (SPSS) program (Version 17.0; SPSS, Chicago, IL). Descriptive statistical analysis was performed to calculate the means with corresponding standard deviation (SD). The test of proportion was used to compare the different proportions, and Chi-square (χ^2) test was performed to find the associations. The various above defined characteristics of SF and OV on CT were individually examined with a chi-square test. The value of $p < 0.05$ was considered to be statistically significant. The sensitivity, specificity, positive and negative predictive value of AP sign was calculated.

Results

The study group consisted of consecutive 102 SF patients, 63 men, and 39 women. The mean age (Mean ± SD) of the patients with SF was 46.26 ± 12.8 years. The control group consisted of 248 consecutive patients, 142 men, and 106 women, with positive comprehensive respiratory viral panel for OV. The mean age (Mean ± SD) of patients was 50.26 ± 13.2 years. There was no statistically significant difference between the age group of SF and OV. Table 1 compares the different characteristics of SF with OV infections on HRCT. Fifty percent of SF infected patients and 75% of OV infected patients showed consolidations, with about 24% of SF and 40% of OV showing bilateral multifocal or diffuse consolidations. Focal nodular infiltrates were more common in OV infections. Of the SF and OV who had GGO, an equal majority (51%) were multifocal asymmetrical. Tree in bud infiltrates, bronchial wall thickening, reticular opacities, and pleural effusions could not differentiate the two. Pneumothorax was present only in two patients with OV infections and was not present in any of the SF patients. One of the SF patients had cavitating consolidation. The AP sign (Figs. 1 and 3–5), when present, could identify 72.5% of patients with SF. It was absent in 49% of patients with OV and was an effective assertor of SF ($p < 0.0004$). The sign had a sensitivity of 72.5%, a specificity of 48%, a positive predictive value of

Table 1. Comparison of various CT findings of SF versus OV infections. The numbers are in percentages. NS = Not statistically significant.

Serial no.	Characteristics	Category	SF (%)	OV infections (%)	*p*-value
1	AP sign (Figs. 1, 3 and 5)	Positive	72.5	51.6	0.0004
2	GGO with or without septal thickening (Figs. 2 and 5)	Unilateral	0.09	0.18	0.06 (NS)
		Bilateral asymmetrical	51.9	51.6	0.99 (NS)
		Bilateral symmetrical	38.2	30.2	0.14 (NS)
3	Consolidation (Fig. 3)	Focal	14.7	23.3	0.93 (NS)
		Multifocal unilateral	9.8	13.7	0.31 (NS)
		Multifocal bilateral/diffuse	24.5	39.5	0.01
4	Nodular infiltrates (Fig. 4)	Focal	21.3	35.1	0.01
		Multifocal unilateral	0.04	0.07	0.24 (NS)
		Multifocal bilateral	27.1	31.6	0.42 (NS)
5	Tree in bud appearance (Fig. 4)	Present	0.01	0.05	0.08 (NS)
6	Reticulation/architectural distortion (Fig. 5)	Present subpleural	0.19	0.20	0.90 (NS)
7	Bronchial wall thickening (Fig. 5)	Present	25	21	0.93 (NS)
8.	Pleural effusion (Figs. 3 and 4)	Unilateral	0.009	0.02	0.06 (NS)
		Bilateral	0.14	0.24	0.95 (NS)
9.	Pneumothorax, cavitation	Present	One case had a cavity	Two cases had pneumothorax	NS

36%, a negative predictive value of 81%, and an accuracy of 55.4%.

Table 2 shows different CT features in various common viral infections. Most of the viral infections frequently cause air space opacifications in the form of ground glass attenuations and consolidations except for metapneumovirus. Centrilobular nodules and tree in bud infiltrate are rarely seen in coronavirus and parainfluenza virus. AP sign is commonly seen in SF, infrequently in entero-rhinovirus and rarely observed in coronavirus and metapneumovirus. Pleural effusions are common in entero rhinovirus which is uncommon in SF.

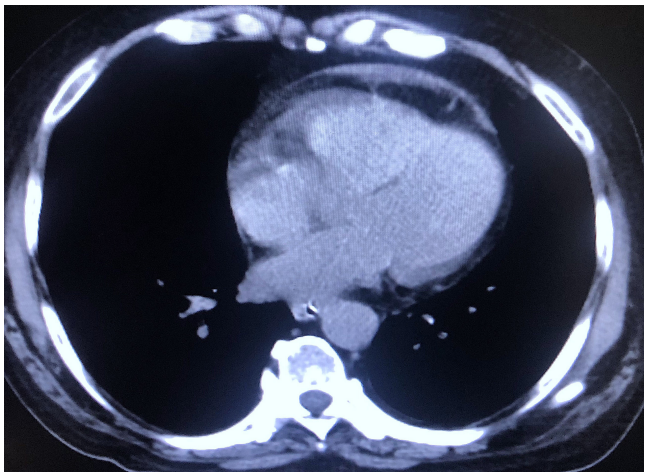


Figure 1. Axial section CT, mediastinal window, with SF, shows thickened pericardium anteriorly consistent with positive AP sign.

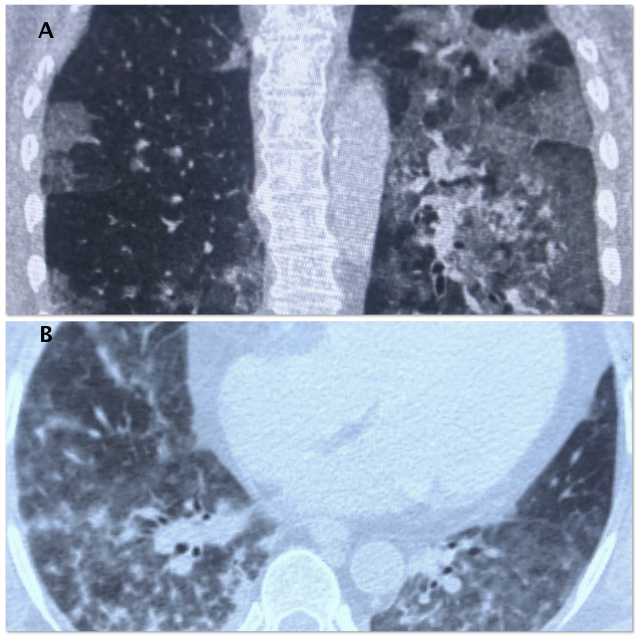


Figure 2. A: Coronal Reconstruction, lung window, in a patient with SF, shows bilateral multifocal asymmetrical GGO. B: Axial section, lung window, shows diffuse GGO in a confirmed case of SF.

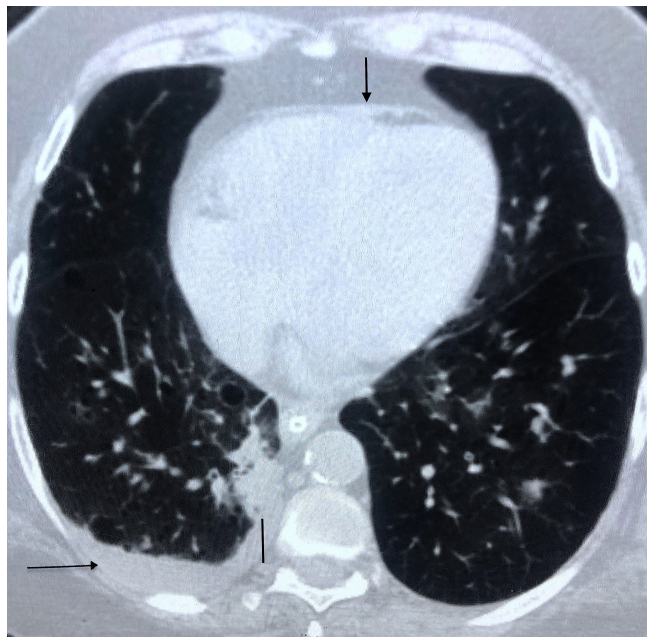


Figure 3. Axial Section HRCT, lung window, in a patient with SF, shows positive AP sign (vertical arrow), mild right pleural effusion (horizontal arrow) and focal patchy peripheral consolidation (line).

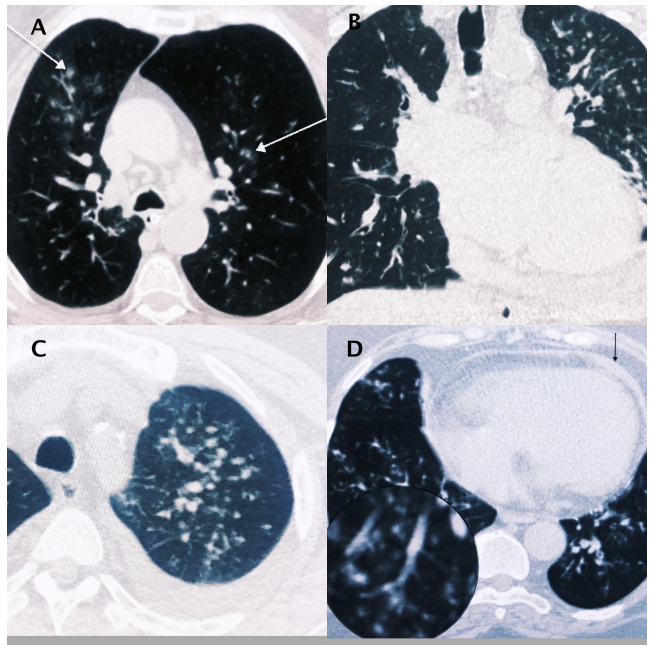


Figure 4. A: Axial section, lung windows, arrows point to centrilobular nodules in case of SF. B: Coronal section of a different patient of SF shows scattered centrilobular nodules. C: Axial section shows pleural effusion and centric lobular nodules in a patient with SF. D: Axial section HRCT, lung window, in a patient with SF, shows positive AP sign (vertical arrow), nodular infiltrates, tree in bud appearance (magnified section).

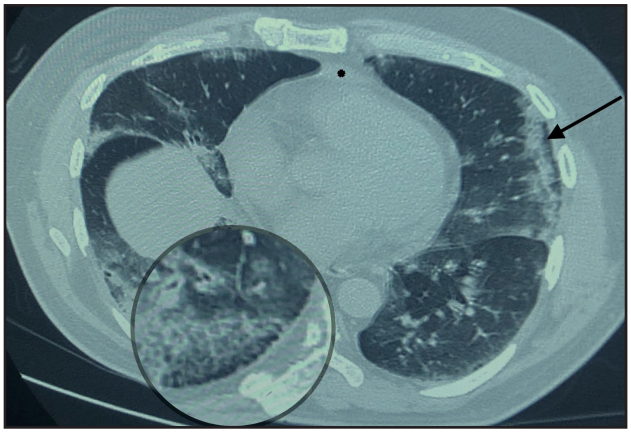


Figure 5. Axial section HRCT, lung window, in a patient with SF, shows positive AP sign (round dot), reticulation and fibrosis (oblique arrow), bronchial wall thickening (upper part of magnified section) and crazy paving pattern (lower part of magnified section).

Mediastinal lymphadenopathy is common is metapneumovirus. The craniocaudal distribution of the lesions in SF and OV was random, with no particular zonal predominance in most of the cases; however, predominant lower lobe involvement is seen in about 30% of the cases of SF. In axial distribution, peripheral lung involvement was more frequent (70%) in SF and coronavirus.

Discussion

We prospectively evaluated CT scans of 102 confirmed cases of H1N1 and 248 cases of OV as a study group and control group, respectively. We tried to establish common computerized tomographic findings and assess the value of the AP sign. The most characteristic findings were GGO (Figs. 2 and 5) and consolidations (Fig. 3), along with a combination of the two in both H1N1 and OV infections. These changes were frequently bilateral, asymmetrical, and multifocal [8,11,12]. Our findings positively correlated with literature. A crazy-paving pattern, in which GGO are associated with septal thickening, has been reported in few cases in the literature [13–15]. In our study, 34% and 39% of the patients showed this pattern with SF and OV infection, respectively. Nodular infiltrates (Fig. 4), be it air space nodules, centrilobular nodules, or perilymphatic nodules, were observed in about 48% of patients with SF and about 66% of patients with OV. Multifocal bilateral was a typical distribution. A study on 10 patients by Tanaka et al. [13] revealed the same about nodular infiltrates. In our sample, pleural effusion was observed in less than 1% of the cases, either in SF or OV, bilateral more common. Pleural effusion, either unilateral or bilateral, is minimal in viral infections and has been described in only some cases [8,11,12].

About one-fourth of our patients of SF and OV showed bronchial wall thickening. In the literature, few studies have described these findings in varying frequencies [12,16]. Only one study has found bronchial wall thickening in all of their patients [16]. Another research suggested that these features occur

Table 2. Different CT features in various common viral infections.

Viruses/CT features	Entero-rhino virus	Adeno virus	Corona virus	Influenza A H1N1	Other Influenza A or B	Parainfluenza virus	Metapneumo virus
GGO/consolidation	MF+++ (50%–75%)	MF+++ (50%–75%)	P+++ (50%–75%)	P+++ (50%–75%)	MF++ (25%–50%)	MF++ (25%–0%)	P+ (10%–25%)
Nodular infiltrates	Centrilobular/ tree in bud +	Centrilobular +	R	Centrilobular/ tree in bud ++	R	R	++
AP sign	++ (25%–50%)	+	R	+++ (50%–75%)	+	+	R
Pleural effusion	F	F	R	R	R	R	F
Mediastinal lymphadenopathy	R	R	R	R	R	R	F
Others like Pneumothorax, pericardial effusion, pulmonary edema, etc.	R	R	R	R	+	R	R

GGO, Ground glass opacities; MF, Multifocal; P, Peripheral; R, Rare; F, Frequent; +, 10%–25% cases; ++, 25%–50% cases; +++, 50%–75% cases; ++++, more than 75% cases.

early in the course of the disease, before the patients seek medical, and is therefore poorly reported [13]. Tanaka et al. [13] related the high occurrence of these changes (68%) to the fact that their study group had easy access to medical management and diagnostic work-up. Similarly, Elicker et al. [16] stated that high prevalence in their study was possibly due to prompt medical attention their patients received, given their comorbidities and immunocompromised status. In contrast, other authors reported, air trapping in the late phase, 3 months after the onset of the disease was related to small airway disease [17]. Air trapping was rare in our cases.

In an overall literature review of HRCT findings of SF, the most frequent distribution of the disease was bilateral multifocal involvement predominantly in the lower lobes [8,12,15,17]. This distribution correlates well with our study. A diffuse pattern without zonal predominance was frequently detected in one study [18]. In our cohort, the HRCT scans showed bilateral involvement in about 90% of the cases with the asymmetrical participation of the lungs in the vast majority (about 60%), similar to Amorim et al. [19]. Data in the literature [8,15,17]. Regarding the axial distribution of HRCT findings commonly depicted peripheral predominance, similar to our study.

The standard pericardial thickness ranges from 0.7 to 2 mm on CT sections [20,21]. The pericardium is considered thickened when the width is 4 mm or more [22]. Inflammation of pericardium causes pericardial thickening, thus the AP sign, which can be diffuse or focal. Although the exact incidence and etiology of pericarditis are challenging to assess, it is commonly idiopathic generally presumed to be viral [22]. The other causes of pericarditis include bacterial, fungal infections, trauma, autoimmune diseases, cancer, radiation, uremia, post-infarction syndrome, side effects of medications, etc. [23]. The pericardial thickening is best assessed anteriorly on CT due to fat density on either side. In our study, we tried to determine the relationship of pericardial thickening in SF as a novel diagnostic sign. This sign is 72.5% sensitive and is statistically significant. There are few reports of pericardial diseases as a complication of SF [24,25]. However, to our knowledge, there is no literature associating AP thickening to SF as a diagnostic imaging tool for SF. COVID-19 is a severe viral lung infection, there are papers on CT features and scoring system of COVID-19 [26], we have not considered in our paper as our data collection is prior to the COVID-19 pandemic.

Conclusion

Differentiation of SF and OV has been challenging thus far on CT with many overlapping findings. We present a new sign, AP sign, which is sensitive for SF with high negative predictive value. This sign can, therefore, help to differentiate SF from OV and to rule out SF with a high degree of confidence. The limitation of this sign is that it is not shown to be specific for SF and is not very accurate. More extensive studies assessing this sign may validate it to be a critical CT marker of SF.

Limitations

Our study had a few limitations. First, there was selection bias. Being a tertiary referral institute, our patients were generally sick, most of them requiring ICU admission, and therefore superadded bacterial infections could contribute to CT findings. Secondly, our study sample is small, a larger multicentric study would be needed to establish AP sign as an added CT feature of viral pneumonia. The third limitation is that the Radiologists were not blinded to the diagnosis of viral pneumonia, raising the possibility of potential reading bias. The fourth limitation is that we did not follow up on the patients nor compared previous imaging, hence the disappearance/persistence of AP thickening found in our patients was due to the present viral infection or not could be conclusively established. To summarize, in a patient with clinical suspicion of viral infection if CT chest shows GGO/consolidation, and centrilobular nodules and thickened anterior pericardium, swine influenza is most likely. However, in cases where CT chest shows pleural effusions, mediastinal lymphadenopathy and absent AP thickening, swine influenza is less likely.

References

[1] Jilani TN, Jamil RT, Siddiqui AH. H1N1 influenza (swine flu). StatPearls Publishing, Treasure Island, FL, 2019. Available via https://www.ncbi.nlm.nih.gov/books/NBK513241/

[2] Kshatriya RM, Khara NV, Ganjiwale J, Lote SD, Patel SN, Paliwal RP. Lessons learnt from the Indian H1N1 (swine flu) epidemic: predictors of outcome based on epidemiological and clinical profile. J Family Med Prim Care 2018; 7(6):1506–9; doi: 10.4103/jfmpc.jfmpc_38_18

[3] Thorner AR. Clinical manifestations, and diagnosis of pandemic H1N1 influenza (swine influenza). Available via http://www.uptodate.com/contents/clinical-manifestations-and-diagnosis-of–pandemic-h1n1-influenza-swine-influenza

[4] Mahony J, Chong S, Merante F, Yaghoubian S, Sinha T, Lisle C, et al. Development of a respiratory virus panel test for detection of twenty human respiratory viruses by use of multiplex PCR and a fluid microbead-based assay. J Clin Microbiol 2007; 45(9):2965–70; doi: 10.1128/JCM.02436-06

[5] Nicolini A, Claudio S, Rao F, Ferrera L, Isetta M, Bonfiglio M. Influenza A (H1N1)-associated pneumonia. J Bras Pneumol 2011; 37(5):621–7.

[6] Cui W, Zhao H, Lu X, Wen Y, Zhou Y, Deng B, et al. Factors associated with death in hospitalized pneumonia patients with 2009 H1N1 influenza in Shenyang, China. BMC Infect Dis 2010; 10:145.

[7] Aviram G, Bar-Shai A, Sosna J, Rogowski O, Rosen G, Weinstein I, et al. H1N1 influenza: initial chest radiographic findings in helping predict patient outcome. Radiology 2010; 255(1):252–9.

[8] Marchiori E, Zanetti G, Hochhegger B, Rodrigues RS, Fontes CA, Nobre LF, et al. High-resolution computed tomography findings from adult patients with influenza A (H1N1) virus-associated pneumonia. Eur J Radiol 2010; 74(1):93–8.

[9] Amorim VB, Rodrigues RS, Barreto MM, Zanetti G, Hochhegger B, Marchiori E. Influenza A (H1N1) pneumonia: HRCT findings. J Bras Pneumol 2013; 39(3):323–9.

[10] Ajlan AM, Quiney B, Nicolaou S, Müller NL. Swine-origin influenza A (H1N1) viral infection: raddiographic and CT findings. AJR 2009; 193:1494–9; doi:10.2214/AJR.09.3625

[11] Li P, Zhang JF, Xia XD, Su DJ, Liu BL, Zhao DL, et al. Serial evaluation of high-resolution CT findings in patients with pneumonia in novel swine-origin influenza A (H1N1) virus infection. Br J Radiol 2012; 85(1014):729–35.

[12] Rodrigues RS, Marchiori E, Bozza FA, Pitrowsky MT, Velasco E, Soares M, et al. Chest computed tomography findings in severe influenza pneumonia occurring in neutropenic cancer patients. Clinics (Sao Paulo) 2012; 67(4):313–8.

[13] Tanaka N, Emoto T, Suda H. High-resolution computed tomography findings of influenza virus pneumonia: a comparative study between seasonal and novel (H1N1) influenza virus pneumonia. Jpn J Radiol 2012; 30:154–61.

[14] Marchiori E, Zanetti G, D'Ippolito G, Hochhegger B. Crazy-paving pattern on HRCT of patients with H1N1 pneumonia. Eur J Radiol 2011; 80(2):573–5.

[15] Henzler T, Meyer M, Kalenka A, Alb M, Schmid-Bindert G, Bartling S, et al. Image findings of patients with H1N1 virus pneumonia and acute respiratory failure. Acad Radiol 2010; 17(6):681–5.

[16] Elicker BM, Schwartz BS, Liu C, Chen EC, Miller SA, Chiu CY, et al. Thoracic CT findings of novel influenza A (H1N1) infection in immunocompromised patients. Emerg Radiol 2010; 17(4):299–307.

[17] Marchiori E, Zanetti G, Mano CM. Swine-origin influenza A (H1N1) viral infection: small airways disease. AJR Am J Roentgenol 2010; 195(4):W317.

[18] Toufen C Jr, Costa EL, Hirota AS, Li HY, Amato MB, Carvalho CR. Follow-up after acute respiratory distress syndrome caused by influenza a (H1N1) virus infection. Clinics (Sao Paulo) 2011; 66(6):933–7.

[19] Amorim VB, Rodrigues RS, Barreto MM, Zanetti G, Hochhegger B, Marchiori E. Influenza A (H1N1) pneumonia: HRCT findings. J Bras Pneumol 2013; 39(3):323–9.

[20] O'Leary SM, Williams PL, Williams MP. Imaging the pericardium: appearances on ECG-gated 64-detector row cardiac computed tomography. Br J Radiol 2010; 83(987):194–205.

[21] Truong MT, Erasmus JJ, Gladish GW. Anatomy of pericardial recesses on multidetector CT: implications for oncologic imaging. AJR Am J Roentgenol 2003; 181(4):1109–13.

[22] Bogaert J, Francone M. Pericardial disease: value of CT and MR imaging. Radiology 2013; 267(2):340–56; doi:10.1128/JCM.02436-06

[23] Imazio M, Gaita F, LeWinter M. Evaluation and treatment of pericarditis: a systematic review. J Am Med Assoc 2015; 314:1498–506.

[24] Jang JY, Chang HJ, Jang Y, Han SH, Bang WD, Cho SS, et al. Constrictive pericarditis accompanied by swine-origin influenza A (H1N1) infection. Korean Circ J 2010; 40(10):539–42.

[25] Martin-Lázaro JF, Homs C, Benito R, Pedro AS, Suárez MA. Chronic pericardial effusion secondary to a influenza virus A (H1N1)/2009 infection. Turk Kardiyol Dern Ars 2013; 41(2):157–60.

[26] Malpani Dhoot N, Goenka U, Ghosh S, Jajodia S, Chand R, Majumdar S, et al. Assigning computed tomography involvement score in COVID-19 patients: prognosis prediction and impact on management. BJR Open 2020; 2:20200024; doi:10.1259/bjro.20200024